COMPARISON OF A ROBUST AND A FLATNESS BASED CONTROL FOR A SEPARATED SHEAR FLOW

Ralf Becker and Rudibert King [1]

Measurement and Control Group, Institute of Process and Plant Technology, Berlin University of Technology, Hardenbergstr. 36a, 10623 Berlin, Germany

Abstract: Closed-loop flow control is gaining more and more interest in the last few years. Whereas most of the published results are based on simulation studies, this work explores the synthesis of black-box model based closed-loop controllers for separated, wall-bounded shear flows in experiments. In this paper we compare a linear robust controller with a flatness based approach. To consider both the uncertainty of the model and the inherent time delay, the well-known flatness based controller synthesis scheme had to be extended by a robust design approach and a prediction step. The actuated backward-facing step flow is chosen as a benchmark configuration, in which the length of the separated flow region is to be controlled. This configuration can be seen as a simple representation of the situation in a burner or behind a flame holder.

Keywords: robust, flatness, time delay, flow control, backward-facing step, separated flow, reattachment length

1. INTRODUCTION

Separated flows show positive and negative effects depending on the application. A desired recirculation region as a result of a separation is needed in combustion chambers to keep the fuel mixture in the reaction zone for a complete combustion. By influencing a recirculation zone, the residence time behaviour in a general mixing problem is altered. In contrast to that, negative consequences could be efficiency loss and noise production in turbomachines and process plants, or drag increase and lift reduction for aeroplanes.

When shaping of the geometry has reached an optimum or when passive means, such as vortex generators, have positive and negative effects, active devices in open- or closed-loop control can further improve the performance by suction and blowing or acoustic actuation. However, most of the work published so far is dedicated to open-loop control.

Experimental validations of closed-loop flow control are still rather rare. The present investigation explores the closed-loop control of separated flows by active means in wind tunnel experiments to profit from the well-known advantages, such as disturbance rejection and set-point tracking. As a benchmark problem, the flow around a backward-facing step is investigated here. For feedback flow control three different approaches concerning the controller synthesis can be distinguished. First, strategies based on a numerical solution of the governing Navier Stokes equations (NSE) are proposed. This is done by (Hinze, 2000), for instance, who also gives a review about this field. How-

[1] Corresponding author: e-mail: Rudibert.King@tu-berlin.de, web: http://mrt.tu-berlin.de

ever, those approaches are still not applicable in real-time. In a second promising approach, low-dimensional models based on the NSE are derived, with the intention to describe the nonlinear physics and to synthesise nonlinear controllers. The use of those Galerkin- and vortex models for controller synthesis and their application to experimental setups is still in a state of research, see e.g. (Baker and Christofides, 2002), (Noack *et al.*, 2003) and (Pastoor *et al.*, 2003). First experimental results are presented in (Glauser *et al.*, 2004) and (Siegel *et al.*, 2004).

Third, (Allan *et al.*, 2000) and (Becker *et al.*, 2005) propose low-dimensional black-box models for controller synthesis as a feasible alternative for experimental configurations. In (Allan *et al.*, 2000) tuning rules are used for the control of a generic model of an airfoil. Robust controllers are synthesised and compared in simulation studies and wind tunnel experiments in (Becker *et al.*, 2005). This approach will be used here as well. A survey of several successful applications of robust and adaptive controllers for separated shear flows is given in (King *et al.*, 2004).

This paper is organised as follows: A description of the configuration and its dynamics is given in section 2. First, a simply structured, linear controller is designed employing robust methods, see section 3. However, the performance is limited by the uncertainty of the linear design model. Second, to overcome this limitation, a nonlinear model that resolves the dynamical phenomena more precisely in combination with a flatness based control approach is proposed in section 4. The command tracking performance of the robust and the flatness based control are compared in section 5. Finally, the results are summarised.

2. FLOW CONFIGURATION

2.1 General description

The backward-facing step flow has been established as a benchmark problem for separated flows in fluid dynamics. A variety of information about the flow process and actuation mechanisms is available, see for example the survey in (Becker *et al.*, 2005). A sketch of the flow field is given in Fig. 1 where the oncoming flow detaches at the edge of the step and reattaches downstream. Three different regimes exist in the wake: a separation region, also called separation bubble, a reattachment zone and a newly developing boundary layer. The separation bubble consists of the recirculation zone and the shear layer above.

Here, the goal is to control the size of the separation bubble given by the reattachment length x_R.

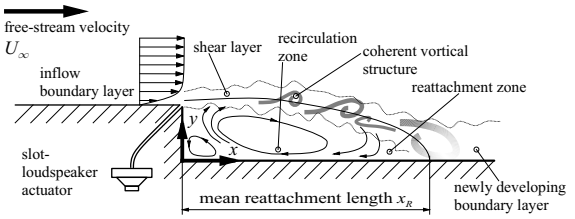

Fig. 1. Flow field downstream of a backward-facing step

While negative skin-friction, i.e. reverse flow, occurs in the recirculation zone, downstream a new boundary layer develops causing positive skin-friction, i.e. forward flow. The reattachment position x_R is characterised by zero friction.

The shear layer above the recirculation zone is governed by the Kelvin-Helmholz instability phenomenon. Perturbations are amplified and lead to two-dimensional shear layer roll-up into spanwise coherent vortical structures which grow and convect downstream. Particularly the vortices are responsible for entrainment of fluid out of the bubble. By stimulating their growth, the increased outflow leads to a significant reduction of the bubble size x_R.

The vortex generated entrainment mechanism is enhanced by acoustic actuation of the detaching boundary layer at the edge of the step as shown in Fig. 1. A slot-loudspeaker actuator is used for this. Therefore, the forcing frequency should be near the natural instability frequency of the system. As the forcing frequency is fixed to the optimal one, the amplitude of the harmonic loudspeaker signal finally affects the initial size of the growing vortices, and thus, the reattachment length x_R. In control notation the amplitude of the loudspeaker signal is taken as the control signal $u(t)$ and the reattachment length as the plant output $y(t) = x_R(t)$.

2.2 Flow parameters

A Reynolds number of $Re_H = 4000$ corresponding to $U_\infty = 3.04\,\mathrm{m/s}$ giving the dimensionless free-stream velocity and a step height of $H = 20\,\mathrm{mm}$ are chosen. To compare the results with fluid dynamical investigations, all distances are made dimensionless by the step height H and all times by the ratio H/U_∞ in the following. Details about the experimental setup are described in (Becker *et al.*, 2005).

An online measurement of the output signal $x_R(t)$ cannot be done in a straightforward manner. In the present investigation, wall pressure fluctuations are measured by a microphone array, and a Kalman filter based scheme is used to estimate the reattachment length $x_R(t)$. Details about this approach can be found in (Becker *et al.*, 2003).

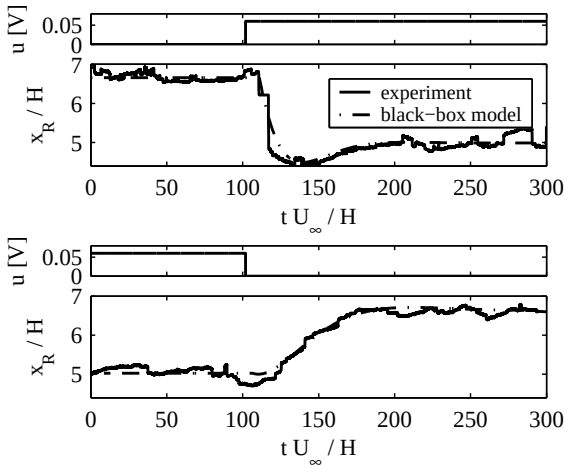

Fig. 2. Identification of black-box models from step responses (*top:* switching $u(t)$ on; *bottom:* switching $u(t)$ off).

2.3 Dynamical behaviour

In spite of the nonlinear and infinite dimensional Navier Stokes equations, it is surprising that the dynamical behaviour of the reattachment length x_R looks very simple in step experiments, see Fig. 2. It can be approximated by stable linear black-box models $G_P(s)$ of first or second order with a time-delay, see again (Becker *et al.*, 2005). Due to the nonlinear characteristics of the investigated system, large ranges for the model parameters have to be accepted for various step heights of the input signal. To avoid a significant detuning of the controller, it is desirable to reduce the model uncertainty. As the steady-state gain $K_P = \lim_{s\to 0} G_P(s)$ of all identified models shows a highly nonlinear dependence on the size of the control signal u, i.e. the forcing amplitude, the inverse f^{-1} of the stationary operating point characteristics $y = K_P(u)u = f(u)$ (u = const., $t \to \infty$) can be used to compensate for this nonlinearity.

In order to describe the nonlinear behaviour of the real process, a family Π of linear black-box models $G_P(s) \in \Pi$ is identified from representative step experiments, see Fig. 3. The spread of the cut-off frequencies is caused by the different dynamics of the experiments with positive, i.e. switching on, and negative, i.e. switching off, steps $u(t)$. However, the slower switching off steps and the faster switching on steps are clustered, respectively.

3. ROBUST CONTROL

Due to the uncertainty of the identified models, robust controllers are required to maintain closed-loop stability for all operating points. A linear nominal model $G_n(s)$ with a multiplicative uncertainty description

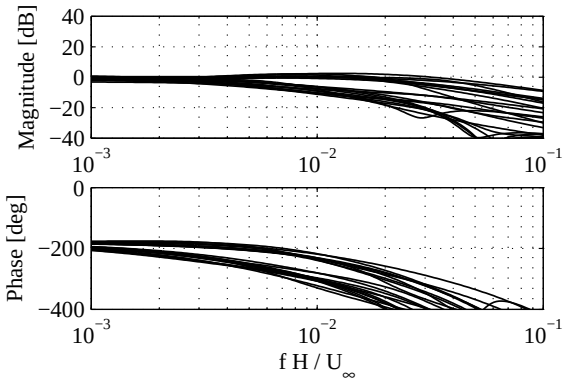

Fig. 3. Frequency responses of the model family with compensation of the nonlinear gain.

$$l_M(\omega) = \max_{G_P \in \Pi} |(G_P(j\omega) - G_n(j\omega))/G_n(j\omega)|$$

for the neglected or non-modelled dynamics is derived from the model family Π, and these are then used for robust controller synthesis. By searching a nominal model $G_n(s)$ with the smallest uncertainty radius, it turnes out that a simple first-order transfer function $G_n(s) = \frac{K}{1+sT} e^{-T_0 s}$ can be used, see as well (Becker *et al.*, 2005). A Padé-approximation of second order is used for the following controller synthesis.

To find a trade-off between the performance, given by the closed-loop sensitivity function, the restriction of the magnitude of the plant input signals, and the robustness, the mixed sensitivity problem is solved by $\mathcal{H}_\infty$-minimisation to shape the closed-loop transfer functions.

The obtained $\mathcal{H}_\infty$-controller is tested in wind tunnel experiments. Comparing the open- and closed-loop tracking responses in the case of switching $u(t)$ on (see first step response after $tU_\infty/H = 90$ in Fig. 4), the closed-loop response shows a slower behaviour than the open-loop response. This can be explained with the wide spread of the cut-off frequencies of $G_P(s) \in \Pi$, see Fig. 3. Due to the requirement of robust stability, the crossover frequency of $l_M(\omega)$ is an upper bound of the active control frequency domain, i.e. the closed-loop gain has to drop below 1 for higher frequencies. However, in this case the crossover frequency of $l_M(\omega)$ is near the lower cut-off frequencies of the clustered models $G_P(s)$ that describe the switching off processes. Hence, the limited validity of the linear nominal model $G_n(s)$, given by $l_M(\omega)$, limits the achievable closed-loop performance to the case of the slowest process behaviour, i.e. the switching off dynamics. Thus, the closed-loop transient time of the first switching on step in Fig. 4 is as slow as in the switching off case. The transient open- and closed-loop velocities are the same after $u(t)$ is switched off. The different transient time after the second step in Fig. 4 is a result of the different starting level due to noise.

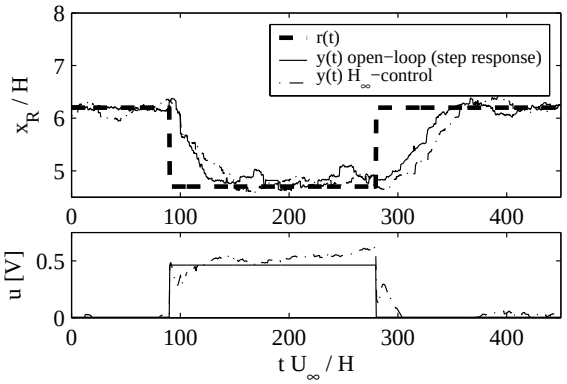

Fig. 4. Comparison between the dynamics of the open-loop and the closed-loop (linear $\mathcal{H}_\infty$-controller) systems with step responses.

Although the linear $\mathcal{H}_\infty$-control shows a slow behaviour, it is superior to open-loop control in the presence of disturbances. The feature of disturbance rejection is demonstrated in the experiments of (Becker *et al.*, 2005).

4. FLATNESS BASED CONTROL

Since the performance limitation of the robust controller is imposed by the uncertainty of the linear design model, an extended model that describes the real behaviour more precisely, in combination with a flatness based control, are proposed next. The idea is to exploit the correlation between the black-box model parameters and the flow state, and to improve the control based on this more precise description.

4.1 Black-box model for the flatness based controller synthesis

The underlying philosophy here is that a more precise description can be obtained by taking the state depending time constants for the switching on and off processes into consideration. To do so, the flow process is empirically described by the following time delay-free system

$$[T + \mathrm{sign}(\dot{y}^*(t))\Delta T]\,\dot{y}^*(t) + y^*(t) = u(t) \qquad (1)$$

and the output time delay

$$y(t) = y^*(t - T_0)\ . \qquad (2)$$

$y^*(t)$ is an artificial system output without time delay. The time constant of the system is chosen depending on the sign of $\dot{y}^*(t)$, i.e. the direction of motion of $y^*(t)$. Thus, the faster responses, after switching $u(t)$ on, are described by the time constant $T - \Delta T$, and the slower responses, after switching $u(t)$ off, by $T + \Delta T$. This accounts for a hysteresis-type effect known for such flow systems. Due to the compensation f^{-1}, see above, the steady-state gain of Eq. (1) is one.

The model (1,2) approximates the process by switching between the two first order models $G_{on}(s)$ and $G_{off}(s)$ according to

$$\begin{aligned} G_{on/off}(s) &= \frac{Y(s)}{U(s)} = \frac{Y^*(s)}{U(s)} e^{-sT_0} \\ &= \underbrace{\frac{1}{1 + (T \mp \Delta T)s}}_{G^*_{on/off}(s)} e^{-sT_0}\ . \end{aligned} \qquad (3)$$

In fact, the time constants of the system responses after non-stepwise changes in $u(t)$ are somewhere between the values $T \pm \Delta T$. Both, the simple first order models and the switching between the two time constants $T \pm \Delta T$ are simplifications of the real behaviour. On the one hand, overshoots and oscillations cannot be described by those PT_1-models. On the other hand, the switching criterium, $\mathrm{sign}(\dot{y}^*(t))$, is a simplification, too, and its evaluation is uncertain due to measurement noise. Concluding these facts, robustness in the sense of the uncertain time constant and of an incorrect switching between $T \pm \Delta T$ is desirable for the control to follow.

4.2 Control

Roughly speaking, a system is differentially flat if it is possible to find an output vector $\mathbf{y} = \mathbf{y}(\mathbf{x}, \mathbf{u}, \dot{\mathbf{u}}, \ldots, \mathbf{u}^{(\alpha)})$ with $\dim \mathbf{y} = \dim \mathbf{u}$, such that all states $\mathbf{x}$ and all inputs $\mathbf{u}$ are expressed by those outputs and a finite number of its derivatives according to $\mathbf{x} = \mathbf{x}(\mathbf{y}, \dot{\mathbf{y}}, \ldots, \mathbf{y}^{(\beta)})$ and $\mathbf{u} = \mathbf{u}(\mathbf{y}, \dot{\mathbf{y}}, \ldots, \mathbf{y}^{(\beta+1)})$. Since the behaviour of the flat system can be parameterised by the flat output $\mathbf{y}$, it is possible to plan trajectories in output space. The basic approach of a two degrees-of-freedom design is to separate the nonlinear controller synthesis problem into the design of a feedforward tracking control, followed by a feedback control for the stabilisation around the desired trajectory in the presence of uncertainties and disturbances. The feedback control is designed such that the tracking error dynamics is linear.

Both the input $u(t)$ and the internal state $y^*(t)$ of the system (1,2) can be parameterised by $y(t)$, i.e.

$$\begin{aligned} u(t) = {} & [T + \mathrm{sign}(\dot{y}(t + T_0))\Delta T]\,\dot{y}(t + T_0) + \\ & + y(t + T_0) \end{aligned} \qquad (4)$$

and

$$y^*(t) = y(t + T_0)\ . \qquad (5)$$

Hence, the physical output $y(t)$ contains the flatness property. Due to the inherent time delay T_0,

$u(t)$ and $y^*(t)$ are parameterised by the future output $y(t+T_0)$. This extension of the concept of flatness to time delay systems is proposed by (Mounier and Rudolph, 1998).

With the control law

$$u(t) = [T + \text{sign}(\underbrace{\dot{y}(t+T_0)}_{\dot{y}^*(t)})\Delta T]\,\underbrace{v(t+T_0)}_{v^*(t)} + \\ + \underbrace{y(t+T_0)}_{y^*(t)} \tag{6}$$

$$\underbrace{v(t+T_0)}_{v^*(t)} = \underbrace{\dot{y}_d(t+T_0)}_{\dot{y}_d^*(t)} - \\ -q(\underbrace{y(t+T_0)}_{y^*(t)} - \underbrace{y_d(t+T_0)}_{y_d^*(t)}) \tag{7}$$

the closed loop reads

$$[T + \text{sign}(\dot{y}^*(t))\Delta T]\,\dot{y}^*(t) + y^*(t) = \\ [T + \text{sign}(\dot{y}^*(t))]\,(\dot{y}_d^*(t) - q(y^*(t) - y_d^*(t))) + y^*(t)$$

The superscript $*$ denotes the future variables at $t+T_0$ that are predicted at time instant t. Introducing the future error $e(t+T_0) = e^*(t) = y^*(t) - y_d^*(t)$ it follows from the above equation that the error equation is linear in the nominal case, according to $\dot{e}^*(t) + qe^*(t) = 0$. The controller design variable q has to be chosen positive, such that $e^*(t)$ decreases to zero, thereby keeping the system (1,2) around the desired trajectory $y_d^*(t) = y_d(t+T_0)$ in the presence of disturbances and model uncertainties.

In the non-nominal case with a time-varying time constant $T_P(t)$ of the real system, stability of the error equation for $T - \Delta T \le T_P(t) \le T + \Delta T$ can be shown. The error $e^*(t)$ tends to zero when $\dot{y}_d^*(t) \to 0$ which is given in all practical problems for the backward facing step.

4.3 Implementation

To implement the above control law (6, 7), the internal state $y^*(t) = y(t+T_0)$ has to be estimated by a prediction. Therefore, the well-known Smith-predictor structure is used, see Fig. 5. A time delay-free model $G^*(s)$ is simulated parallel to the process to predict $y^*(t)$. Depending on the sign of $d\hat{y}^*(t)/dt$, $G^*(s)$ is chosen according to $G^*(s) = G^*_{on}(s)$ (switching on process) or $G^*(s) = G^*_{off}(s)$ (switching off process), respectively. In the Smith-predictor approach the nominal model $G^*(s)e^{-sT_0}$ is simulated as well parallel to the process. In the nominal case with $d = 0$, $y(t)$ and the output of $G^*(s)e^{-sT_0}$ cancel such that the prediction $y^*(t) = \hat{y}^*(t)$ of $G^*(s)$ is used as feedback, and the control system behaves as if the time delay is arranged after the control structure according to $y(t) = y^*(t - T_0)$. One price payed

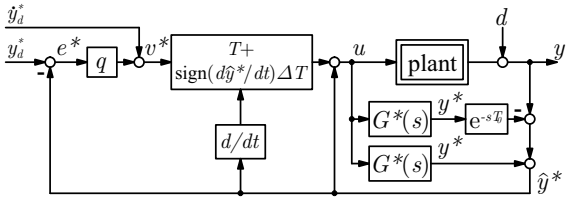

Fig. 5. Extension of the flatness based control (6, 7) to predict the internal state $y^*(t) = y(t+T_0)$ online and in real-time.

using the Smith-predictor is that the feedback signal consists of the prediction of the future output $y^*(t) = y(t+T_0)$ superimposed by actual disturbances $d(t)$ and signal components resulting from model mismatch, i.e. of a corrected signal $\hat{y}^*(t)$. This results in a performance limitation of the feedback control for disturbance rejection. An alternative prediction approach is proposed by (Mounier and Rudolph, 1998).

4.4 Robust design

In order to analyse the closed-loop stability not with model (3), but with a better description using the identified model family $G_P \in \Pi$, the loop transfer functions

$$L_P(j\omega) = \frac{\hat{Y}^*(j\omega)}{E(j\omega)} \\ = qT_n \frac{G_P(j\omega) + G^*(j\omega)(1 - e^{-j\omega T_0})}{1 - G_P(j\omega) - G^*(j\omega)(1 - e^{-j\omega T_0})} \tag{8}$$

are evaluated by the Nyquist criterium. $T_n = T \pm \Delta T$ denotes the nominal time constant. The goal is to guarantee both robust stability in the sense of uncertainties of the model and of incorrect switching between $G^*(s) = G^*_{on}(s)$ and $G^*(s) = G^*_{off}(s)$, and between $T_n = T - \Delta T$ and $T_n = T + \Delta T$. The controller gain q is chosen such that $L_P(j\omega)$ in the 'worst case' does not encircle the critical point -1. To do so, all possible loop transfer functions $L_P(j\omega)$, i.e. all combinations between $G^*(s)$ and T_n for the two nominal cases, respectively, and the models $G_P(s) \in \Pi$ of the family are considered. In order to obtain a high performance, q is designed as high as possible.

Since the feedback loop only stabilises the tracking of the reference $y_d^*(t)$, its performance limitation does not limit the feedforward command tracking performance. The 'worst case' crossover frequency of $L_P(j\omega)$ is a measure for the disturbance rejection performance, and this is approximatively as twice as high in comparison to the robust $\mathcal{H}_\infty$-control. This is due to both the different control structures and the more conservative unstructured uncertainty description applied in the $\mathcal{H}_\infty$-design.

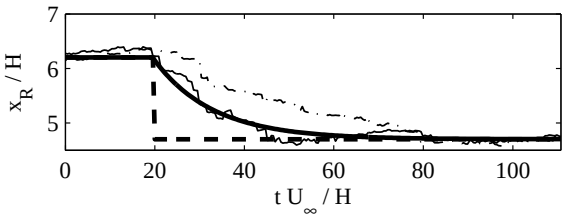

$\mathcal{H}_\infty$-control:		flatness based control:	
— —	$r(t)$	———	$y_d(t) = y_d^*(t - T_0)$
— · —	$y(t)$	———	$y(t)$

Fig. 6. Comparison between the dynamics of the linear $\mathcal{H}_\infty$-controller and the flatness based controller with closed-loop step responses.

5. COMMAND TRACKING PERFORMANCE RESULTS OF BOTH CONTROLS

A comparison of the command tracking responses of both controls is displayed in Fig. 6. Both, the inherent time delay T_0 and the uncertainty $l_M(\omega)$ of the linear design model $G_n(s)$ limit the performance of the robust control, resulting in a transport delay of $T_0 U_\infty / H = 8$ convective time units after the stepwise decrease of $r(t)$ and the following slow transient behaviour. However, the flatness based control can compensate for the delay by an appropriate choice of the future reference $y_d^*(t) = y_d(t + T_0)$. Since the flatness based control splits command tracking and disturbance rejection, the feedforward control is not limited. Consequently, even faster references $y_d^*(t)$ could be followed. Only the disturbance rejection performance is limited by the time delay and the uncertainty of the design model $G^*(s)$.

6. CONCLUSIONS

A fast and cheap controller synthesis for the separated flow around a backward facing step can be performed employing robust methods such as $\mathcal{H}_\infty$-controller design. However, the inherent time delay and the uncertainty of the linear design model imposes a limitation on the achievable performance, i.e. the performance is limited to the case of the slowest process behaviour.

A faster command tracking performance can be obtained by a nonlinear design model that resolves the different state depending dynamics of the flow process in combination with a flatness based control. Although the nonlinear design model contains significant uncertainties, an arbitrary fast command tracking performance can be achieved due to the splitting between open-loop command tracking and closed-loop disturbance rejection. Two extensions had to be added to the classical flatness based control design scheme. First, as the control signal is computed from the future output, the prediction approach of the well-known Smith predictor was used for the online computation in real-time. Second, the feedback control for disturbance rejection was designed to guarantee robust stability. One price paid is that in contrast to the $\mathcal{H}_\infty$-controller, a lot of experience for the determination of the nonlinear black-box design model and its uncertainty description is needed.

REFERENCES

Allan, B.G., J.-N. Juang, D.L. Raney, A. Seifert, L.G. Pack and D.E. Brown (2000). Closed-loop separation control using oscillatory flow excitation. *Technical Report NASA/CR-2000-210324, ICASE Report No. 2000-32.*

Baker, J. and P.D. Christofides (2002). Drag reduction in transitional and linearized channel flow using distributed control. *Inter. J. Contr.* **75**, 1213–1218.

Becker, R., M. Garwon and R. King (2003). Development of model-based sensors and their use for closed-loop control of separated shear flows. In: *Proc. of the European Control Conference ECC 2003.* University of Cambridge, UK.

Becker, R., M. Garwon, C. Gutknecht, G. Bärwolff and R. King (2005). Robust control of separated shear flows in simulation and experiment. *Journal of Process Control, accepted for publication.*

Glauser, M.N., H. Higuchi, J. Ausseur and J. Pinier (2004). Feedback control of separated flows. *AIAA-Paper 2004-2521.*

Hinze, M. (2000). Optimal and instantaneous control of the instationary Navier-Stokes equations. Habilitation thesis. Technische Universität Berlin. Berlin.

King, R., R. Becker, M. Garwon and L. Henning (2004). Robust and adaptive closed-loop control of separated shear flows. *AIAA-Paper 2004-2519.*

Mounier, H. and J. Rudolph (1998). Flatness based control of nonlinear delay systems: a chemical reactor example. *Int. J. Control* **71**, 871–890.

Noack, B.R., K. Afanasiev, M. Morzynski, G. Tadmor and F. Thiele (2003). A hierarchy of low-dimensional models of the transient and post-transient cylinder wake. *J. Fluid Mech.* **497**, 335–363.

Pastoor, M., R. King, B.R. Noack and A. Dillmann (2003). Model-based coherent-structure control of turbulent shear flows using low-dimensional vortex models. *AIAA-Paper 2003-4261.*

Siegel, S., K. Cohen and T. McLaughlin (2004). Experimental variable gain feedback control of a circular cylinder wake. *AIAA-Paper 2004-2611.*